Published OnlineFirst November 11, 2014; DOI: 10.1158/0008-5472.CAN-14-0629

Tumor and Stem Cell Biology

Cancer Research

SYK Is a Candidate Kinase Target for the Treatment of Advanced Prostate Cancer

Veerander P.S. Ghotra[1], Shuning He[2], Geertje van der Horst[3], Steffen Nijhoff[1], Hans de Bont[1], Annemarie Lekkerkerker[4], Richard Janssen[4], Guido Jenster[5], Geert J.L.H. van Leenders[6], A. Marije M. Hoogland[6], Esther I. Verhoef[6], Zuzanna Baranski[1], Jiangling Xiong[1], Bob van de Water[1], Gabri van der Pluijm[3], B. Ewa Snaar-Jagalska[2], and Erik H.J. Danen[1]

Abstract

Improved targeted therapies are needed to combat metastatic prostate cancer. Here, we report the identification of the spleen kinase SYK as a mediator of metastatic dissemination in zebrafish and mouse xenograft models of human prostate cancer. Although SYK has not been implicated previously in this disease, we found that its expression is upregulated in human prostate cancers and associated with malignant progression. RNAi-mediated silencing prevented invasive outgrowth *in vitro* and bone colonization *in vivo*, effects that were reversed by wild-type but not kinase-dead SYK expression. In the absence of SYK expression, cell surface levels of the progression-associated adhesion receptors integrin α2β1 and CD44 were diminished. RNAi-mediated silencing of α2β1 phenocopied SYK depletion *in vitro* and *in vivo*, suggesting an effector role for α2β1 in this setting. Notably, pharmacologic inhibitors of SYK kinase currently in phase I–II trials for other indications interfered similarly with the invasive growth and dissemination of prostate cancer cells. Our findings offer a mechanistic rationale to reposition SYK kinase inhibitors for evaluation in patients with metastatic prostate cancer. *Cancer Res; 75(1); 230–40. ©2014 AACR.*

Introduction

Prostate cancer is the most common cancer in males and the second leading cause of cancer deaths among men in the Western world (1). Nondetectable micro-metastatic disease may be present in up to 40% of patients (2) while 8% to 14% may have visible or symptomatic bone metastases at diagnosis (3). Although the majority of prostate cancers are diagnosed as organ-confined disease, which is curable by prostatectomy or radiation therapy, 20% to 25% of patients will experience relapse within 5 years of treatment (4). Androgen deprivation therapy is used when prostate cancer reappears, but in most cases, resistance develops within 1 to 3 years. Chemotherapy, particularly docetaxel, is able to prolong overall survival in these cases but it also causes significant toxicity and not all patients receive this therapy. To more successfully combat prostate cancer, screening programs for early diagnosis and treatment of localized disease are important. In addition, some alternatives for docetaxel as first-line treatment for metastatic disease and options for those cases where docetaxel failed have become available (5). Nevertheless, once the disease has spread beyond the prostate, no curative treatments are currently available (6). Hence, there is an urgent need for novel targeted therapies to improve treatment of metastatic prostate cancer.

SYK is a nonreceptor tyrosine kinase containing two adjacent Src homology 2 (SH2) domains, a kinase domain, but no SH3 domain. SYK is expressed in hematopoietic cells where it binds phosphorylated immunoreceptor tyrosine-based activation motifs (ITAM) to mediate immune receptor signaling (7). For malignant hematopoietic cells that rely on immune receptor-mediated survival signals, SYK might represent an attractive drug target. Indeed, pharmacologic inhibition of SYK has shown promising results in the context of non-Hodgkin lymphoma and leukemias (8). SYK is also widely expressed in a variety of cell types outside the hematopoietic system and it is required for proper development of blood and lymph vessels during embryonic development (9, 10). The role of SYK in epithelial cancers appears diverse. SYK abundance negatively correlates with breast cancer progression and SYK suppresses tumor growth and metastasis in breast cancer xenografts (11, 12). Conversely, SYK levels in head and neck squamous cell carcinomas and lymph node metastases are high compared with corresponding normal tissue and SYK promotes migration of squamous carcinoma cells (13). SYK has not been implicated in prostate cancer.

In the current study, we find that SYK adenoviral shRNAs interfere with PC3 human prostate cancer dissemination using a semiautomated whole animal bioimaging platform (14). Further investigations of SYK in patient cohorts, three-dimensional (3D) *in vitro* cultures, and zebrafish and mouse xenografts indicate

[1]Division of Toxicology, Leiden Academic Center for Drug Research, Leiden University, Leiden, the Netherlands. [2]Department of Molecular Cell Biology, Institute of Biology, Leiden University, Leiden, the Netherlands. [3]Department of Urology, Leiden University Medical Center, Leiden, the Netherlands. [4]Galapagos BV, Leiden, the Netherlands. [5]Department of Urology, Erasmus University Medical Center, Rotterdam, the Netherlands. [6]Department of Pathology, Erasmus University Medical Center, Rotterdam, the Netherlands.

Note: Supplementary data for this article are available at Cancer Research Online (http://cancerres.aacrjournals.org/).

Corresponding Authors: Erik H.J. Danen, Division of Toxicology, Leiden Academic Center for Drug Research, Leiden University, Einsteinweg 55, 2333 CC Leiden, the Netherlands. Phone: 31715274486; Fax: 31715274277; E-mail: e.danen@lacdr.leidenuniv.nl; and B. Ewa Snaar-Jagalska, E-mail: b.e.snaar-jagalska@biology.leidenuniv.nl

doi: 10.1158/0008-5472.CAN-14-0629

Published OnlineFirst November 11, 2014; DOI: 10.1158/0008-5472.CAN-14-0629

that SYK may represent a novel candidate drug target for further study in prostate cancer.

Materials and Methods

Cell lines, antibodies, and pharmacologic inhibitors

LNCaP, PC3, DU-145, and HEK293T cells were obtained from ATCC and cultured for fewer than 6 months after receipt or resuscitation according to the provided protocol. ATTC characterized the cell lines using short tandem repeat profiling. PC3-derived PC3-M-Pro4luc cells (15) and LNCaP-derived cell lines C4-2 and C4-2 B were grown in DMEM and T-Medium, respectively. For FACS, primary antibodies included AIIB2 anti-human integrin β1, 4A10 anti-human integrin α2, and sc-18849 anti-human CD44 (Santa Cruz Biotechnology). Goat-anti-mouse APC and donkey-anti-rat PE (Jackson laboratories) were used as secondary antibodies. For IHC in patient tumor samples and Western blot analysis, rabbit anti-human SYK monoclonal antibody (clone EP573Y, ab40781; Abcam) was used. For Western blot analysis, anti-human AKT (#4691; Cell Signaling Technology), anti-phospho-Ser473 AKT (#9271; Cell Signaling Technology), anti-human CD44 MAb (kindly provided by Dr. Marcel Spaargaren, Academic Medical Center, Amsterdam, the Netherlands), and α-tubulin (B-5-1-2; Sigma) were used. R-406 and BAY-61-3606 were obtained from Selleckchem and Sigma, respectively.

Zebrafish xenotransplantation experiments

For quantification of tumor cell spreading, tumor cells were labeled with CM-DiI (Invitrogen), mixed with 2% PVP, and injected into the yolk sac of enzymatically dechorionated, 2-day-old Casper fli-EGFP transgenic zebrafish embryos using an air-driven microinjector (20 psi, PV820 Pneumatic PicoPump; World precision Inc). Embryos were maintained in egg water at 34°C for 6 days and subsequently fixed with 4% paraformaldehyde. Imaging was done in 96-well plates containing a single embryo per well using a Nikon Eclipse Ti confocal laser-scanning microscope. Z stacks (12 × 30 μm) were obtained using a Plan Apo 4X Nikon dry objective with 0.2 NA and 20 mm WD. Images were converted into a single Z projection in Image-Pro Plus (Version 6.2; Media Cybernetics). Automated quantification of tumor cell spreading per embryo, cumulative distance of cells per embryo, and mean cumulative distance (MCD) for all embryos was determined using an in-house built Image-Pro Plus plugin as previously described (14).

Transient adenoviral shRNA transduction

PC3 cells were transduced one day after seeding with adenoviral shRNA constructs from Galapagos BV (Leiden) using a multiplicity of infection of 15 for 24 hours. After 3 days, medium was replaced and after an additional 2 days, the transduced PC3 cells were detached with trypsin and single cell suspensions were used for zebrafish xenotransplantation.

Stable shRNA and cDNA expression

PC3 or PC3-M-Pro4luc cells were transduced using Sigma's MISSION library lentiviral shRNAs (shSYK#1: TRCN0000003167, shSYK#2:TRCN0000199566; shITGB1#1:TRCN0000029645, shITGB1#2:TRCN0000029646; shITGA2#1: TRCN0000057730, shITGA2#2: TRCN000000057731). For lentivirus production, HEK293T cells were transfected with the short hairpin constructs together with the packaging plasmids REV, GAG, and VSV in a 1:1:1:1 ratio using PE (Sigma) as transfection reagent. Lentiviral supernatant was collected 48 hours after transfection and used for transduction or target cells in the presence of 8 μg Polybrene (Sigma). Transduced cells were bulk selected in medium containing 2 μg/mL puromycin. Lentiviral shRNA vector targeting TurboGFP was used as a negative control. Retroviral cDNAs for wild-type and kinase dead SYK were a gift from Drs. Wei Zou and Steven Teitelbaum, Washington University, St Louis, MO (16). Retrovirus was produced in Plat-E packaging cells and used for transduction of PC3-M-Pro4-luc cells stably expressing shRNA targeting SYK 3′ untranslated region (UTR), followed by bulk blasticidin selection.

mRNA expression analysis

For qPCR, total RNA was extracted using RNA easy Plus Mini Kit (Qiagen). cDNA was randomly primed from 50 ng total RNA using iScript cDNA Synthesis Kit (Bio-Rad) and real-time qPCR was subsequently performed in triplicate using SYBR green PCR (Applied Biosystems) on a 7900HT fast real-time PCR system (Applied Biosystems). The following qPCR primer sets were used:
GAPDH: forward *AGCCACATCGCTCAGACACC*, reverse *ACCCGTTGACTCCGACCTT*;
SYK forward *GATGCTGGTTATGGAGATG*, reverse *TCTATGATGTTCTTATCCTTGAC*;
CD44 forward *TGGCACCCGCTATGTCCAG*, reverse *GTAGCAGGGATTCTGTCTG*;
ITGB1 forward *ATTGACCTCTACTACCTT*, reverse *GTGTTGTGCTAATGTAAG*;
ITGA2 forward *AACTCTTTGGATTTGCGTGTG*, reverse *TGGCAGTCTCAGAATAGGCTTC*.

Data were collected and analyzed using SDS2.3 software (Applied Biosystems). Relative mRNA levels after correction for GAPDH control mRNA were expressed using $2^{(-\Delta\Delta Ct)}$ method.

For mRNA expression analysis of human prostate cancer patient material either directly or following xenografting in mice, existing datasets were queried as described (17).

Colony formation assay

Cells were seeded into a 96-well plate containing approximately 1 cell per well. After 1 to 3 weeks, percentage of wells showing colonies and colony size was determined by microscopy (Zeiss Axiovert 200M).

3D invasion assays

Cell suspensions in PBS containing 2% polyvinylpyrrolidone (PVP; Sigma-Aldrich) were microinjected (~1×10^4 cells/droplet) using an air-driven microinjector (20 psi, PV820 Pneumatic PicoPump; World precision Inc) into solidified 3D collagen gels in 8-well μslides (IBIDI) as previously described (18). Collagen gels were prepared from 2.5 mg/mL acid-extracted rat tail collagen type I. Collagen was diluted to working concentration of 1 mg/mL in complete medium containing 44 mmol/L NaHCO3 (stock 440 mmol/L, Merck) and 0.1 mol/L Hepes (stock 1 mol/L, BioSolve). Tumor cell spheroids were monitored for approximately 1 week using Nikon eclipse TS100. For immunostaining, gels were incubated for 1 hour with 5 μg/mL collagenase (Clostridium histolyticum, Boehringer Mannheim) at room temperature, fixed with 4% paraformaldehyde, and permeabilized in 0.2% Triton X-100. After fixation, collagen gels were stained using a cocktail containing 4% paraformaldehyde, 0.2% Triton X-100 (Sigma), and 0.1 μmol/L rhodamine phalloidin (Sigma) for 3 hours. Thereafter, wells were washed with PBS. Preparations were then mounted in

Published OnlineFirst November 11, 2014; DOI: 10.1158/0008-5472.CAN-14-0629

Aqua-Poly/Mount solution (Polysciences, Inc) and imaged using a Plan Apo 4X Nikon dry objective with 0.2 NA and 20 mm WD. A total of 15 Z planes at an interval of 30 μm were captured. Image stacks were converted into two-dimensional maximum intensity projections using ImagePro 7.0. Cell spheroids were analyzed using an automated Image pro 7-based plugin to calculate surface area of spheroid, number of cells migrating out of the cell spheroid, and cumulative distance travelled by these cells.

Immunohistochemistry

Immunohistochemistry (IHC) was performed on a series of formalin-fixed, paraffin-embedded radical prostatectomies and prostate lymph node metastases. Five micron sections were dewaxed and rehydrated using xylene and ethanol. Endogenous peroxidase was blocked in 0.3% H_2O_2 and antigen retrieval was performed under pressure (0.9 bar) in TRIS-EDTA buffer (pH = 9, Klinipath). SYK antibody (ab40781, Abcam) was diluted 1:300 in normal antibody diluent (Scytek) and incubated overnight at 4°C. Envision (DAKO) was used to visualize the antibody, counterstaining was performed with hematoxylin. The percentage and intensity (negative 0, weak 1+, moderate 2+, strong 3+) of positive SYK staining were estimated in benign luminal epithelial cells and prostate adenocarcinoma. Lymphocytes served as internal positive control in all prostate and lymph node samples. Mann–Whitney *U* testing was performed to compare median expression levels.

Experimental bone metastasis assay

Male nude (BALB/c nu/nu) mice were anesthetized and injected with a single-cell suspension of 10^5 cells/100 μL in PBS into the left cardiac ventricle. Outgrowth of spread PC3-M-Pro4-luc cells was monitored weekly by whole body bioluminescent imaging (BLI) using an intensified charge-coupled device video camera of the *in vivo* Imaging System (IVIS100; Xenogen) as described previously (15). Values are expressed as RLUs in photons/second. Bone metastases in a subset of mice were also examined by Goldner staining after mice were sacrificed using decalcified bone.

Flow cytometry and Western blot analysis

For flow-cytometry, surface expression levels were determined using primary antibodies, followed by fluorescence-conjugated secondary antibodies, and analysis on a FACSCanto or sorting on a FACSCalibur (Becton Dickinson). For Western blot analysis, cells were lysed with modified RIPA buffer (150 mmol/L NaCl, 1.0% triton-X 100, 0.5% Na deoxycholate, 0.1% 50 mmol/L Tris, pH 8, and protease cocktail inhibitor; Sigma-Aldrich). Samples were separated by SDS-PAGE and transferred to polyvinylidene difluoride membranes (Millipore), incubated with primary antibodies then horseradish peroxidase-labeled secondary antibodies (Jackson ImmunoResearch Laboratories, Inc.), and developed with enhanced chemiluminescence substrate mixture (ECL plus, Amersham, GE Healthcare). Blots were scanned on a Typhoon 9400 (GE Healthcare).

Statistical analysis

Data are presented as mean ± SEM of at least three independent biologic replicates unless otherwise stated. Student *t* test (two tailed) was used to compare groups except for IHC on human prostatectomies and lymph node metastasis where Mann–Whitney *U* testing was used to compare the median expression levels between groups.

Results

Identification and validation of SYK in prostate cancer zebrafish xenografts

A panel of human prostate cancer cell lines was xenografted in the yolk of zebrafish embryos and dissemination was analyzed using a whole animal automated bioimaging platform as described (14). Prostate cancer cell lines reported to be androgen independent and/or metastatic in mice (LnCaP-derived C4-2 and C4-2B; DU145 and PC3) showed enhanced dissemination in comparison with androgen-dependent nonmetastatic LnCAP cells (Supplementary Fig. S1A–S1D; refs. 19–22).

As a first step toward an adenovirus-based RNAi screening platform for regulators of prostate cancer dissemination, we used adenoviruses targeting two genes previously implicated in prostate cancer (Fig. 1A). These were the CD44 cell surface hyaluronan receptor and the SRC tyrosine kinase (23–26). In addition, the SYK tyrosine kinase was included because it plays apparently opposite roles in different epidermal malignancies and has not been analyzed in prostate cancer (11–13). In agreement with their reported link to growth and progression of prostate cancer, targeting CD44 or SRC, each by two independent shRNAs and in two independent experiments using approximately 25 embryos per condition, led to a significant reduction in PC3 spreading throughout the embryos (Fig. 1B and C). Interestingly, these criteria were also fulfilled for SYK (Fig. 1B and C and Supplementary Fig. S2).

Stable expression of either of two independent lentiviral SYK shRNAs further confirmed the effect of *SYK* gene silencing in the zebrafish xenograft model (Fig. 1D–F). Reduced SYK protein expression in the presence of lentiviral shSYK was confirmed by Western blot analysis and by IHC on agar embedded cells, using the same antibody as used for IHC on human tissue sections (Supplementary Fig. S3A and S3B). Reduced SYK abundance also effectively blocked migration in a model where cell spheroids are embedded in 3D extracellular matrix (ECM) scaffolds (Fig. 1G and H and Supplementary Fig. S4A; ref. 18). In addition, *SYK* gene silencing attenuated spheroid expansion *in vitro* and tumor outgrowth at the primary injection site in zebrafish xenografts (Fig. 1G and H and Supplementary Fig. S2 and S4A). No signs of increased nuclear fragmentation in SYK-depleted spheroids were observed, pointing to decreased proliferation rather than cell death as the underlying mechanism (Supplementary Fig. S4B). We also analyzed the effect of silencing SYK on the ability of PC3 cells to form colonies when plated as single cells *in vitro* (Supplementary Fig. S5A). Reduced SYK levels led to a significant decrease in colony number and size. This was not associated with an apparent decrease in PI3K/AKT signaling because shSYK did not affect AKT phosphorylation on Ser473 reporting AKT activity (Supplementary Fig. S5B). These findings point to a role for SYK in growth and migration of PC3 prostate cancer cells.

Expression of SYK in human prostate cancer

On the basis of these findings, we next analyzed SYK expression levels in human prostate cancer. Breast cancer cells with reported low and high levels of SYK mRNA expression were used as controls (27, 28). Compared with LnCaP, mRNA expression was increased in the androgen-independent LNCaP-derived C4-2 and C4-2B sublines and in DU145 and PC3 androgen-independent, metastatic prostate cancer cell lines (Fig. 2A). Likewise, in a series of human prostate cancer xenografts (29), SYK mRNA

Published OnlineFirst November 11, 2014; DOI: 10.1158/0008-5472.CAN-14-0629

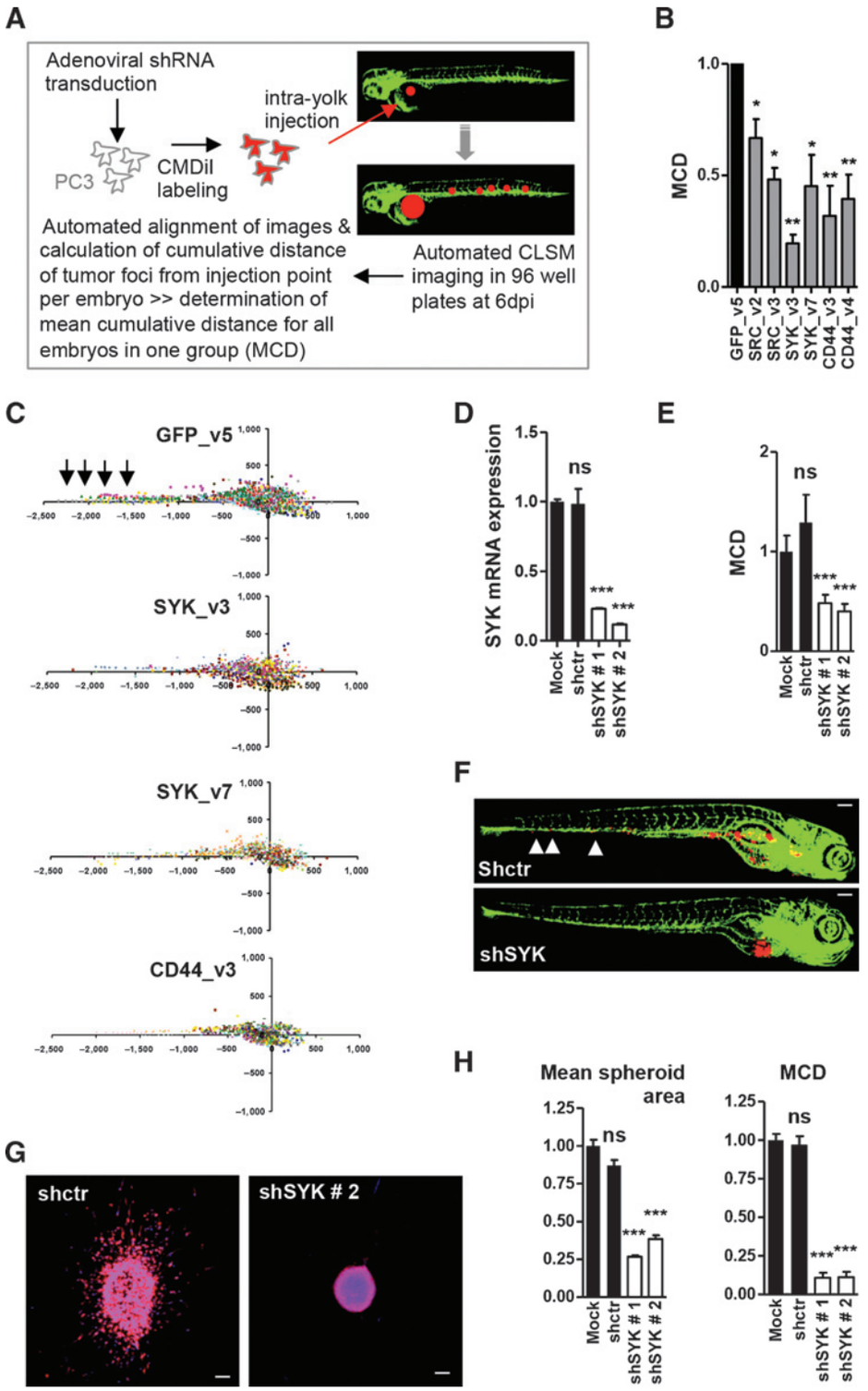

Figure 1.
SYK supports growth, invasion, and dissemination of human prostate cancer cells. A, schematic overview of the *in vivo* screening procedure. B, MCD of tumor foci relative to site of injection for PC3 cells transiently transduced with indicated adenoviral shRNAs calculated from >40 xenografts obtained from two independent experiments. C, representative scatter plots showing tumor foci detected by automated confocal imaging and automated image analysis as described (14) in zebrafish injected with PC3 cells expressing indicated adenoviral shRNAs. Each color shows foci detected in one embryo. Arrows, foci in tail region. D, qPCR verification of SYK silencing in PC3 cells expressing two independent lentiviral shSYK vectors. E and F, MCD (E) and representative images (F) for dissemination in zebrafish of PC3 cells stably expressing indicated lentiviral SYK shRNAs (combined data from two independent experiments using >32 embryos per condition are shown; arrowheads, tumor foci in tail region). G and H, representative images (G) and quantification of expansion (mean spheroid area) and ECM invasion (MCD; H) for control and shSYK PC3 cell spheroids at 6 days postinjection in collagen gels (blue, Hoechst; red, phalloidin). Scale bars, 100 μm. ns, nonsignificant; *, $P < 0.05$; **, $P < 0.01$; ***, $P < 0.005$.

expression was higher in androgen-independent tumors (Fig. 2B). Moreover, SYK RNA expression in prostate cancer metastasis resection specimens was significantly increased compared with primary prostate cancer in two different datasets (Fig. 2C). The EMC dataset used had Gene Expression Omnibus (GEO) number: GSE41410 (30); the Taylor dataset had GEO number GSE21032 (31). The expression of SYK was also compared between normal adjacent prostate (NAP) and primary prostate

Published OnlineFirst November 11, 2014; DOI: 10.1158/0008-5472.CAN-14-0629

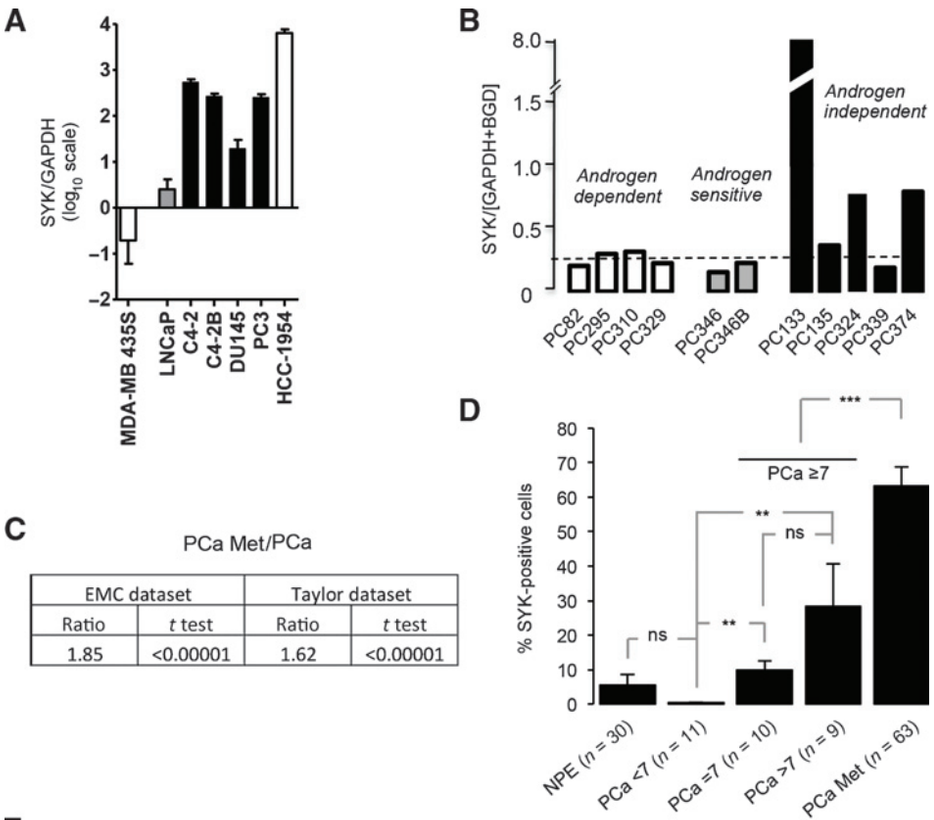

C

PCa Met/PCa

EMC dataset		Taylor dataset	
Ratio	*t* test	Ratio	*t* test
1.85	<0.00001	1.62	<0.00001

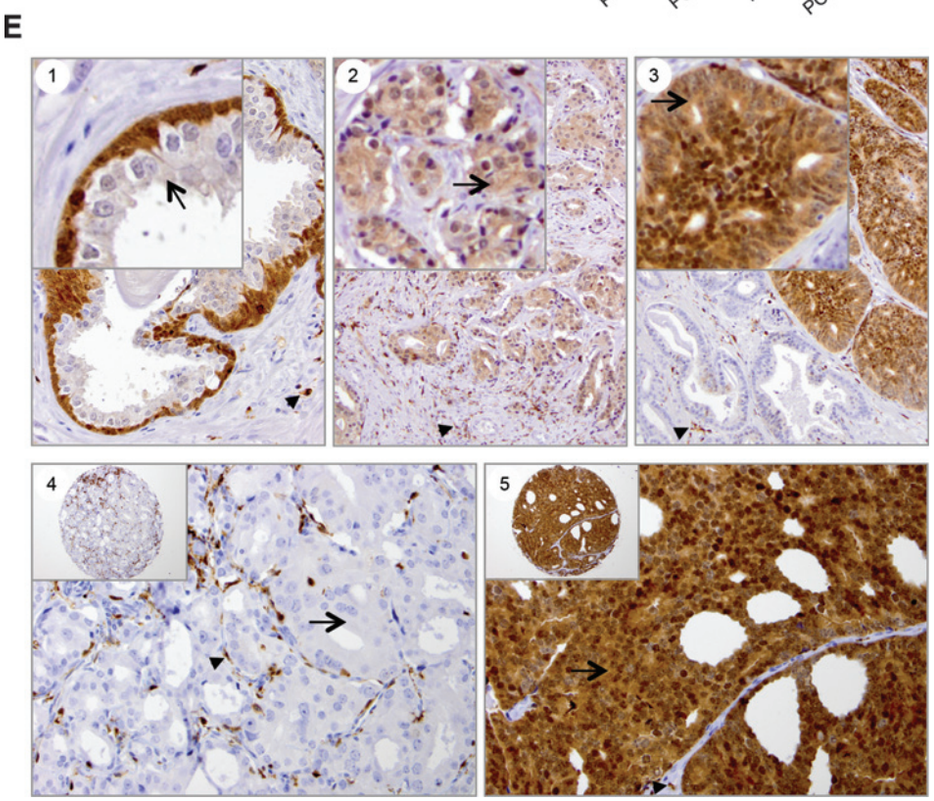

Figure 2.
SYK is expressed in human prostate cancer. A, SYK RNA expression determined by qPCR in indicated cell lines. MDA-MB-435S (hypermethylated SYK gene promoter; refs. 27, 28) and HCC-1954 breast cancer cells (high SYK expression; ref. 28) were used as negative and positive controls, respectively. B, SYK RNA expression in human prostate cancer resection specimens xenografted in mice. C, ratio between SYK RNA expression in prostate cancer metastases [prostate cancer (PCa) Met] and primary prostate cancers and significance (*t* test) in two different datasets. D, semiquantitative analysis (mean and SEM) of SYK expression in normal luminal epithelium, primary prostate cancer, and prostate cancer lymph node metastases. E, IHC detection of SYK in human benign glandular prostate epithelium (1; note staining of basal but rarely of luminal cells), prostate adenocarcinoma (2, weak; and 3, moderate SYK expression), and prostate lymph node metastasis (4, negative; and 5, strong SYK expression). Arrows point to prostate epithelial/cancer cells. Original magnifications, ×200 (1, 4, 5) and ×100 (2, 3). Strong staining in lymphocytes served as internal positive control in all cases (arrowheads). ns, nonsignificant; **, $P < 0.005$; ***, $P < 0.001$ (Mann–Whitney *U* test).

Published OnlineFirst November 11, 2014; DOI: 10.1158/0008-5472.CAN-14-0629

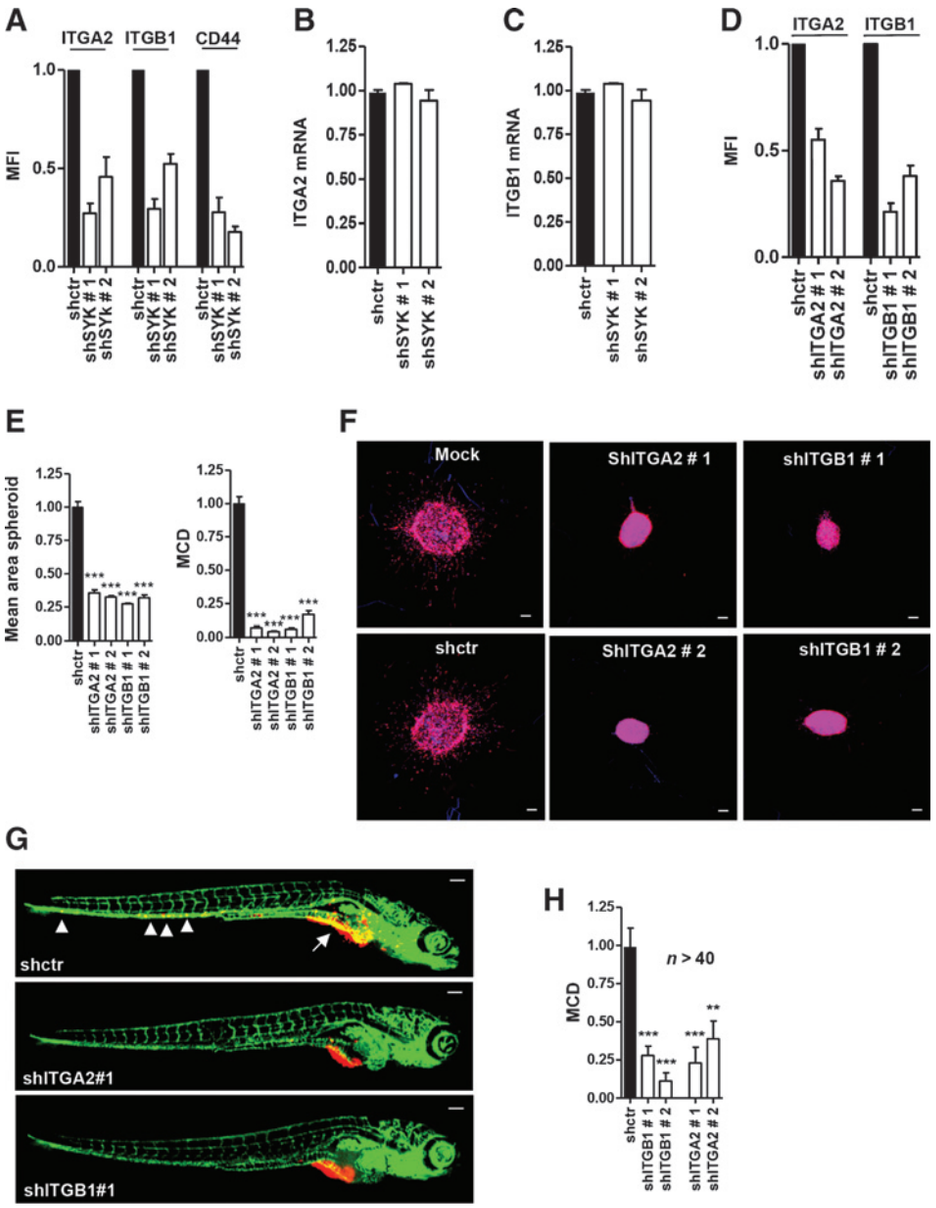

Figure 3.
SYK regulation of adhesion receptor surface expression in human prostate cancer cells modulates invasive outgrowth *in vitro* and dissemination in zebrafish and metastatic colonization in mice. A, FACS analysis of surface expression of CD44 and integrin subunits α2 (ITGA2) and β1 (ITGB1) in PC3 cells expressing control or SYK shRNAs. MFI, mean fluorescence intensity. B and C, qPCR analysis of ITGA2 and ITGB1 mRNA expression in PC3 cells expressing control or SYK shRNAs. D, FACS verification of ITGA2 and ITGB1 silencing in PC3 cells expressing two independent lentiviral vectors targeting ITGA2 or ITGB1, respectively. E and F, quantification of expansion (mean spheroid area) and ECM invasion (MCD; E) and representative images (F) for control, shITGA2, and shITGB1 PC3 cell spheroids at 6 days postinjection in collagen gels (blue, Hoechst; red, phalloidin). G and H, representative images (G) and quantification of MCD (H) for dissemination in zebrafish of PC3 cells expressing indicated lentiviral shRNAs (combined data from two independent experiments using >40 embryo's per condition are shown; arrowheads, tumor foci in tail region). Scale bars, 100 μm. **, $P < 0.01$; ***, $P < 0.005$.

cancer and in both datasets, there was no significant difference in expression between NAP and prostate cancer [prostate cancer/NAP ratios: 0.97 (EMC), 0.94 (Taylor)]. This was further confirmed in the Brase dataset (GEO number GSE29079; ref. 32) where the prostate cancer/NAP ratio was 1.01. These findings indicated that SYK is unlikely to play a role in the early prostate cancer development but rather may have a role in progression of the disease.

Because the stromal compartment may affect mRNA analysis in clinical samples, SYK protein expression was analyzed subsequently in a set of radical prostatectomies for human prostate adenocarcinoma and lymph node metastases. SYK expression was variable in prostate adenocarcinoma ranging from complete absence of staining to moderate (2+) staining in the majority of tumor cells. Expression of SYK in normal luminal glandular epithelium and low-grade prostate cancer (Gleason score <7) did not differ significantly (Fig. 2D). Notably, in preexistent epithelial glands, SYK was expressed in basal cells while luminal cells were only rarely weakly positive (Fig. 2E). Intermediate (Gleason score 7) and high-grade (Gleason score 8-10) prostate cancer demonstrated significantly higher expression of SYK than normal luminal epithelium or low-grade (Gleason score <7) prostate cancer (Fig. 2D and E). SYK expression in prostate cancer lymph node metastasis ranged from undetectable to 100% moderate (2+) staining (Fig. 2E). Median SYK expression in all metastases was significantly higher than that in all intermediate and high-grade primary prostate cancers taken together (Fig. 2D). These results further supported the notion that SYK expression is associated with progression, rather than early development of prostate cancer.

Published OnlineFirst November 11, 2014; DOI: 10.1158/0008-5472.CAN-14-0629

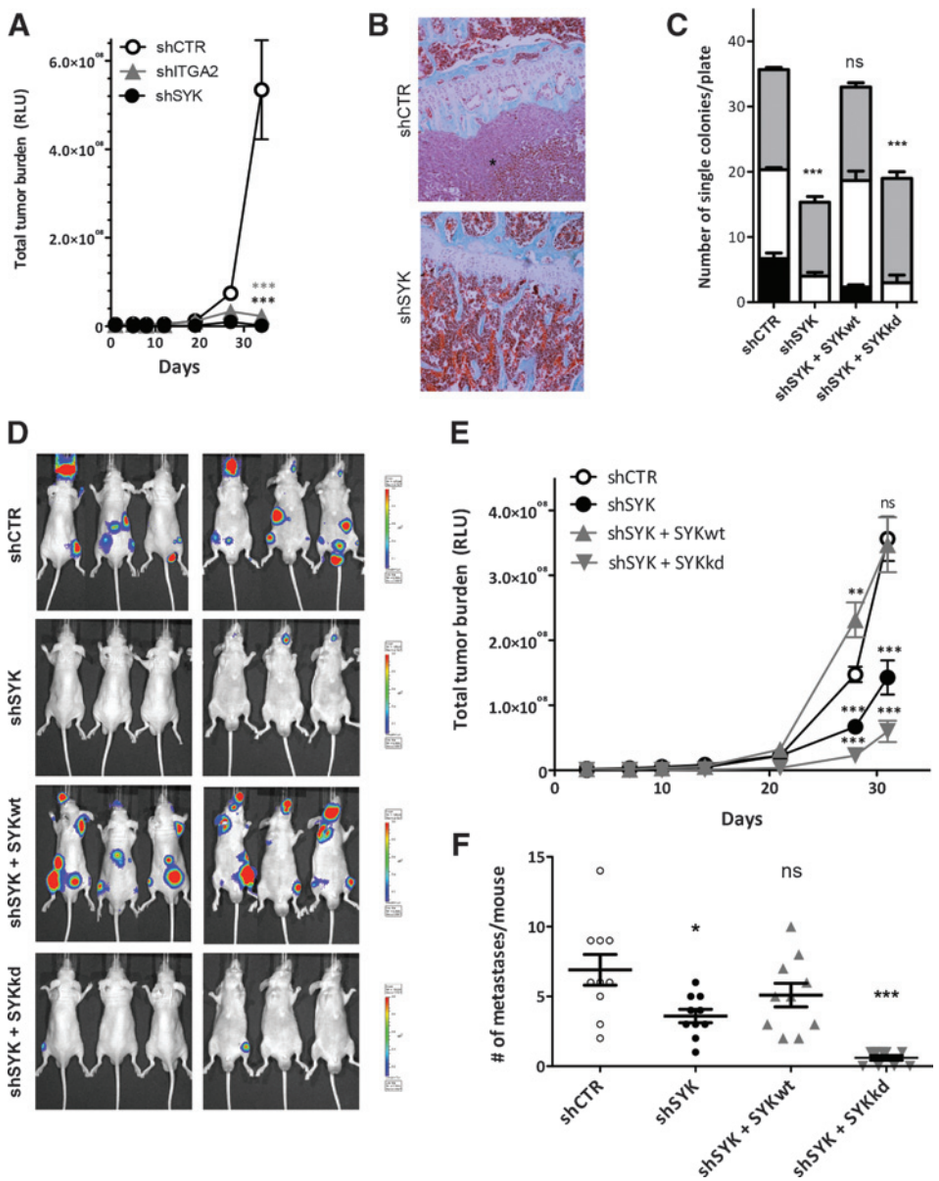

Figure 4.
SYK kinase activity supports metastatic bone colonization in mice. A, total metastatic tumor burden determined by BLI monitoring at indicated time points following intracardiac inoculation in immune-compromised mice for PC3M-Pro4luc variants expressing indicated lentiviral shRNAs (data obtained from at least 9 mice per experimental group). B, bones of mice collected 31 days after intracardiac inoculation with PC3M-Pro4-luc shCTR or shSYK cells and stained with Goldner staining. *, tumor lesion. C, quantification of colony formation assay for PC3M-Pro4-luc cells expressing control or SYK shRNAs in combination with wild-type (SYKwt) or kinase dead SYK (SYKkd) expression vectors. Gray, small; white, medium; black, large colonies. D, BLI images of PC3M-Pro4luc variants expressing control or SYK shRNAs in combination with wild-type (SYKwt) or kinase dead (SYKkd) expression vectors taken 31 days following intracardiac inoculation. E and F, quantification of the experiment shown in D where total metastatic tumor burden was determined by BLI monitoring at indicated time points (E) and the number of metastatic colonies was determined by counting of BLI foci at 31 days following intracardiac inoculation (data obtained from at least 10 mice per experimental group; F). ns, nonsignificant; *, $P < 0.05$; **, $P < 0.01$; ***, $P < 0.005$ versus shCTR.

SYK supports cell surface expression of CD44 and integrin α2β1

In acute myeloid leukemia, inhibition of SYK promotes differentiation (33). We analyzed a set of transcripts previously associated with undifferentiated characteristics of prostate cancer cells (34) but observed no gross changes in the expression of these genes upon depletion of SYK. However, although mRNA levels of the prostate cancer progression-associated markers CD44 and integrin α2β1 (23, 24, 35–37) were unaffected, their cell surface expression, but not total CD44 or integrin β1 protein levels, was suppressed following SYK silencing (Fig. 3A–C and Supplementary Fig. S5C and data not shown). SYK has been previously reported to regulate surface expression of transmembrane receptors (38, 39) and two adenoviral CD44 shRNAs decreased PC3 dissemination in zebrafish (Fig. 1B). Moreover, lentiviral silencing of α2 or β1 integrin subunits, each by two independent shRNAs, suppressed invasive outgrowth in 3D ECM as well as dissemination in the zebrafish xenograft model (Fig. 3D–H). Together, these results identify regulation of surface expression of adhesion receptors as a potential underlying mechanism for the support of prostate cancer dissemination by SYK.

SYK kinase activity supports formation of bone metastases

We next addressed the role of SYK in a preclinical mouse xenograft model for prostate cancer bone metastasis. This preclinical *in vivo* model has been extensively characterized and the PC-3M-Pro4luc cells were selected, by multiple *in vivo* passaging, for extremely high bone tropism (which reflects castration-resistant prostate cancer with bone metastasis in advanced prostate cancer patients) and virtually exclusively colonize bone (marrow; ref. 15). Depletion of SYK led to a strong reduction in metastatic bone tumor burden following intracardiac inoculation of PC3M-

Published OnlineFirst November 11, 2014; DOI: 10.1158/0008-5472.CAN-14-0629

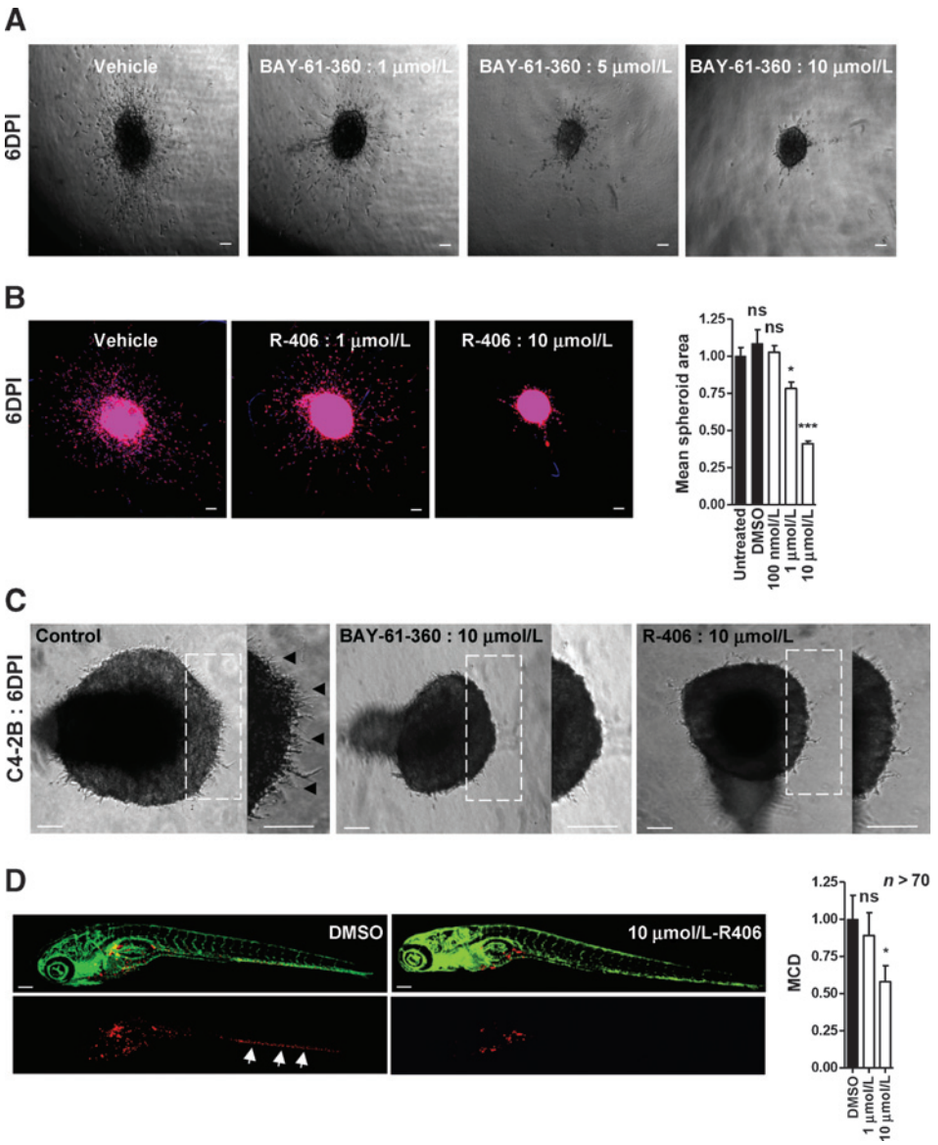

Figure 5.
Pharmacological inhibition of SYK prevents growth, invasion, and dissemination of prostate cancer cells. A, bright field images showing PC3 spheroids 6 days postinjection into collagen gels in the absence or presence of the indicated concentrations of BAY-61-360 (one of three experiments is shown). B, representative images and quantification of expansion (mean spheroid area) and ECM invasion (MCD) for PC3 cell spheroids measured at 6 days postinjection in collagen gels and treated with indicated concentrations of R-406 (blue, Hoechst; red, phalloidin). C, brightfield images showing C4-2B cell spheroids at 6 days postformation in the absence or presence of the indicated concentrations of SYK inhibitors. Arrowheads point to ECM invading strands seen under control conditions, which are not observed in presence of inhibitors. D, representative images and quantified MCD for dissemination in zebrafish of PC3 cells in the absence or presence of indicated concentrations of R-406. Combined data from two independent experiments using >70 embryos per condition are shown. Arrows, cells disseminated to tail region. Scale bars, 120 μm; ns, nonsignificant; *, $P < 0.05$; ***, $P < 0.005$.

Pro4luc cells (Fig. 4A and B). Similar to its effect *in vitro* and in zebrafish xenografts, shRNA targeting the integrin α2-subunit mRNA, phenocopied shSYK in this model (Fig. 4A). To interrogate the specific role for SYK kinase activity in colony formation and prostate cancer bone colonization, wild-type or kinase dead SYK was expressed in PC3M-Pro4luc cells expressing an shRNA targeting the SYK 3′UTR. The reduced capacity to form colonies as well as colony growth in PC3M-Pro4luc-shSYK cells was restored to control levels by wild-type but not kinase dead SYK (Fig. 4C). Moreover, effective bone colonization of shSYK cells was restored by wild-type SYK, whereas expression of kinase dead SYK even further suppressed the process with very few detectable metastases (Fig. 4D–F).

Pharmacologic inhibition of SYK prevents *in vitro* invasion and *in vivo* dissemination

On the basis of the dependency on SYK kinase activity determined in the mouse model, we performed initial experiments to evaluate whether pharmacologic inhibition of SYK could interfere with *in vitro* invasive outgrowth and *in vivo* dissemination using zebrafish xenografts. Small-molecule inhibitors of SYK are in clinical development for autoimmune diseases and lymphoid malignancies (8, 40). Two of these compounds, R-406 and BAY-61-3606, show efficacy in preclinical leukemia and retinoblastoma studies (33, 41–44). When used at 1 to 10 μmol/L, the concentration widely used *in vitro* (33, 41–44), these compounds reduced spheroid outgrowth and ECM invasion of PC3 as well as C4-2B cells (Fig. 5A–C). Moreover, R-406 significantly inhibited dissemination of PC3 cells (Fig. 5D) without significant signs of toxicity at 10 μmol/L (e.g., no effects were observed when yolk sac edema, cardiac edema, bending of the tail, hepatic necrosis, and impaired cardiovascular function were compared for R-406 and vehicle control-treated animals). Thus, pharmacologic inactivation of SYK recapitulated the effect of silencing the SYK gene *in vitro* and in zebrafish xenografts.

Published OnlineFirst November 11, 2014; DOI: 10.1158/0008-5472.CAN-14-0629

Discussion

There is an urgent need for further insights into aspects of prostate cancer progression that provide new avenues for targeted therapy. Our study demonstrates that a semiautomated whole animal bioimaging assay based on zebrafish xenotransplantation (14) can be productive in RNAi-based preclinical prostate cancer drug target discovery. Efficacy of human prostate cancer cell spreading throughout the embryo correlates with androgen independence, a major hallmark of prostate cancer progression, and with behavior in rodent models. Two signaling proteins, previously associated with prostate cancer progression, Src and CD44, are effectively identified using adenoviral shRNAs (23–26). Although the pipeline is currently only partly automated, screening of small adenoviral RNAi sublibraries (~100 genes) is feasible. Integration of the established automated imaging and quantitative image analysis with recently described methods for automated injection and sorting of zebrafish embryos can widen applicability to larger scale screening (45).

Our findings indicate that the protein tyrosine kinase, SYK, supports growth and migration of prostate cancer cells. The evidence comes from two transiently expressed adenoviral and two stably expressed and bulk-sorted lentiviral shRNA vectors. In addition, expression of wild-type SYK rescues the attenuated *in vitro* clonogenic outgrowth and *in vivo* formation of bone metastases of shSYK cells, further arguing against off-target effects. This suggests that the role of SYK in prostate cancer is opposite to its proposed "progression suppressor" role in breast cancer (11, 12). In further support of that, we show that expression of SYK is somewhat increased in more aggressive prostate cancer cell lines and in metastases as compared with primary prostate cancer lesions. A wider analysis of SYK protein expression and activity in a large cohort of patients with prostate cancer will be needed to firmly establish if SYK is positively correlated to progression of prostate cancer, as it appears to be for head and neck squamous cell carcinoma (13).

In hematopoietic cells, immune receptors provide the ITAM for recruitment and activation of SYK. In the epithelial cell types where SYK is expressed, it has not been established whether and how SYK may be activated. Src family kinases are responsible for the ITAM phosphorylation that is required to recruit SYK (7, 46). Src has been associated with prostate cancer progression and RNAi targeting Src also interfered with PC3 dissemination in the zebrafish model. Src may act on a large number of substrates in prostate cancer cells. One potential target in the context of SYK activation that we evaluated was "migration and invasion enhancer 1" (Mien1; also termed C35/C17orf37). Expression of Mien1 is correlated with progression of breast, ovarian, and colon cancer, it contains an ITAM, and it has been reported to require SYK for its breast cancer promoting activity (47–51). However, stable silencing of MIEN1 in PC3 cells did not affect outgrowth or invasion in 3D cultures, indicating that this is unlikely to be involved in prostate cancer growth or invasion (not shown). Further studies will address additional possible mechanisms in the context of prostate cancer.

It is not known how SYK contributes to, or in the case of breast cancer, interferes with tumor progression but modulation of NF-κB activity may be one aspect involved (52). In immune cells, SYK mediates the activation of MAPK signaling, calcium fluxes, and cytoskeletal remodeling when immune receptors are engaged (7, 46). In addition, SYK has been previously reported to support the surface expression of integrins (38, 39). Our findings indicate that stimulation of α2β1 and CD44 cell surface expression may play a role in the stimulation by SYK of invasive growth in 3D ECM *in vitro* and dissemination in the zebrafish model. A role for β1 integrins in intravascular locomotion of MDA-MB-435 breast cancer cells in zebrafish has been previously reported (53). In our study, silencing either α2 or β1 subunits prohibits effective migration in the zebrafish. Moreover, silencing α2β1 phenocopies the effect of silencing SYK in the experimental mouse bone metastasis model. Thus, SYK-mediated stimulation of the cell surface expression of adhesion receptors may contribute to aspects of prostate cancer progression.

Our experiments using a kinase-dead mutant show that stimulation of clonogenic growth *in vitro* and experimental bone metastasis in the mouse depend on SYK kinase activity. Moreover, R-406 and BAY-61-3606 SYK kinase inhibitors that were effective in preclinical leukemia and retinoblastoma studies (33, 41–44) interfere with invasive growth in 3D ECM *in vitro* and dissemination in the zebrafish model. So, genetic or pharmacologic inactivation of SYK kinase activity inhibits invasive growth and dissemination of prostate cancer. We verify that SYK mRNA and protein are detected in human prostate cancer tissues and SYK inhibitors have already been tested in phase I–II clinical trials for other diseases. Altogether, this establishes SYK as a potential new drug target in prostate cancer for which existing pharmacologic inhibitors with known toxicological profiles can be tested for clinical efficacy.

Disclosure of Potential Conflicts of Interest

No potential conflicts of interest were disclosed.

Authors' Contributions

Conception and design: V.P.S. Ghotra, S. He, S. Nijhoff, R. Janssen, Z. Baranski, J. Xiong, G. van der Pluijm, B.E. Snaar-Jagalska, E.H.J. Danen

Development of methodology: S. He, S. Nijhoff, H. de Bont, A. Lekkerkerker, R. Janssen, A.M.M. Hoogland, G. van der Pluijm, B.E. Snaar-Jagalska, E.H.J. Danen

Acquisition of data (provided animals, acquired and managed patients, provided facilities, etc.): S. He, G. van der Horst, S. Nijhoff, H. de Bont, A. Lekkerkerker, R. Janssen, G. Jenster, G.J.L.H. van Leenders, A.M.M. Hoogland, E.I. Verhoef, G. van der Pluijm, B.E. Snaar-Jagalska, E.H.J. Danen

Analysis and interpretation of data (e.g., statistical analysis, biostatistics, computational analysis): V.P.S. Ghotra, G. van der Horst, H. de Bont, A. Lekkerkerker, R. Janssen, G.J.L.H. van Leenders, A.M.M. Hoogland, E.I. Verhoef, G. van der Pluijm, B.E. Snaar-Jagalska, E.H.J. Danen

Writing, review, and/or revision of the manuscript: V.P.S. Ghotra, S. He, G. van der Horst, A. Lekkerkerker, R. Janssen, G. Jenster, E.I. Verhoef, B. van de Water, G. van der Pluijm, B.E. Snaar-Jagalska, E.H.J. Danen

Administrative, technical, or material support (i.e., reporting or organizing data, constructing databases): A. Lekkerkerker, E.I. Verhoef, G. van der Pluijm, B.E. Snaar-Jagalska

Study supervision: R. Janssen, G. van der Pluijm, B.E. Snaar-Jagalska, E.H.J. Danen

Acknowledgments

The authors thank Drs. Wei Zou and Steven Teitelbaum for kindly providing SYK plasmids, Dr. Marcel Spaargaren for the CD44 antibody, Dr. Rene Bottcher for bioinformatics analysis of Syk expression in the different datasets, and Lizette Haazen for technical assistance.

Grant Support

This work was supported by grants from EU FP7 (HEALTH-F2-2008-201439) and Dutch Cancer Society (UL-2010-4670).

The costs of publication of this article were defrayed in part by the payment of page charges. This article must therefore be hereby marked *advertisement* in accordance with 18 U.S.C. Section 1734 solely to indicate this fact.

Received March 5, 2014; revised October 14, 2014; accepted October 20, 2014; published OnlineFirst November 11, 2014.

References

1. Nelson WG, De Marzo AM, Isaacs WB. Prostate cancer. N Engl J Med 2003; 349:366–81.
2. Freedland SJ, Humphreys EB, Mangold LA, Eisenberger M, Dorey FJ, Walsh PC, et al. Risk of prostate cancer-specific mortality following biochemical recurrence after radical prostatectomy. JAMA 2005;294: 433–9.
3. Landis SH, Murray T, Bolden S, Wingo PA. Cancer statistics, 1999. CA Cancer J Clin 1999;49:8–31, 1.
4. Wirth MP, See WA, McLeod DG, Iversen P, Morris T, Carroll K. Bicalutamide 150 mg in addition to standard care in patients with localized or locally advanced prostate cancer: results from the second analysis of the early prostate cancer program at median followup of 5.4 years. J Urol 2004; 172:1865–70.
5. Drake CG, Sharma P, Gerritsen W. Metastatic castration-resistant prostate cancer: new therapies, novel combination strategies and implications for immunotherapy. Oncogene 2013;33:5053–64.
6. Mundy GR. Metastasis to bone: causes, consequences and therapeutic opportunities. Nat Rev Cancer 2002;2:584–93.
7. Turner M, Schweighoffer E, Colucci F, Di Santo JP, Tybulewicz VL. Tyrosine kinase SYK: essential functions for immunoreceptor signalling. Immunol Today 2000;21:148–54.
8. Friedberg JW, Sharman J, Sweetenham J, Johnston PB, Vose JM, Lacasce A, et al. Inhibition of Syk with fostamatinib disodium has significant clinical activity in non-Hodgkin lymphoma and chronic lymphocytic leukemia. Blood 2010;115:2578–85.
9. Abtahian F, Guerriero A, Sebzda E, Lu MM, Zhou R, Mocsai A, et al. Regulation of blood and lymphatic vascular separation by signaling proteins SLP-76 and Syk. Science 2003;299:247–51.
10. Coopman PJ, Mueller SC. The Syk tyrosine kinase: a new negative regulator in tumor growth and progression. Cancer Lett 2006;241:159–73.
11. Toyama T, Iwase H, Yamashita H, Hara Y, Omoto Y, Sugiura H, et al. Reduced expression of the Syk gene is correlated with poor prognosis in human breast cancer. Cancer Lett 2003;189:97–102.
12. Coopman PJ, Do MT, Barth M, Bowden ET, Hayes AJ, Basyuk E, et al. The Syk tyrosine kinase suppresses malignant growth of human breast cancer cells. Nature 2000;406:742–7.
13. Luangdilok S, Box C, Patterson L, Court W, Harrington K, Pitkin L, et al. Syk tyrosine kinase is linked to cell motility and progression in squamous cell carcinomas of the head and neck. Cancer Res 2007;67:7907–16.
14. Ghotra VP, He S, de Bont H, van der Ent W, Spaink HP, van de Water B, et al. Automated whole animal bio-imaging assay for human cancer dissemination. PLoS ONE 2012;7:e31281.
15. van den Hoogen C, van der Horst G, Cheung H, Buijs JT, Pelger RC, van der Pluijm G. Integrin alphav expression is required for the acquisition of a metastatic stem/progenitor cell phenotype in human prostate cancer. Am J Pathol 2011;179:2559–68.
16. Zou W, Reeve JL, Zhao H, Ross FP, Teitelbaum SL. Syk tyrosine 317 negatively regulates osteoclast function via the ubiquitin-protein isopeptide ligase activity of Cbl. J Biol Chem 2009;284:18833–9.
17. Martens-Uzunova ES, Jalava SE, Dits NF, van Leenders GJ, Moller S, Trapman J, et al. Diagnostic and prognostic signatures from the small non-coding RNA transcriptome in prostate cancer. Oncogene 2012;31: 978–91.
18. Truong HH, de Sonneville J, Ghotra VP, Xiong J, Price L, Hogendoorn PC, et al. Automated microinjection of cell-polymer suspensions in 3D ECM scaffolds for high-throughput quantitative cancer invasion screens. Biomaterials 2012;33:181–8.
19. Thalmann GN, Anezinis PE, Chang SM, Zhau HE, Kim EE, Hopwood VL, et al. Androgen-independent cancer progression and bone metastasis in the LNCaP model of human prostate cancer. Cancer Res 1994;54:2577–81.
20. Shevrin DH, Kukreja SC, Ghosh L, Lad TE. Development of skeletal metastasis by human prostate cancer in athymic nude mice. Clin Exp Metastasis 1988;6:401–9.
21. Wu TT, Sikes RA, Cui Q, Thalmann GN, Kao C, Murphy CF, et al. Establishing human prostate cancer cell xenografts in bone: induction of osteoblastic reaction by prostate-specific antigen-producing tumors in athymic and SCID/bg mice using LNCaP and lineage-derived metastatic sublines. Int J Cancer 1998;77:887–94.
22. Ware JL, Paulson DF, Mickey GH, Webb KS. Spontaneous metastasis of cells of the human prostate carcinoma cell line PC-3 in athymic nude mice. J Urol 1982;128:1064–7.
23. Paradis V, Eschwege P, Loric S, Dumas F, Ba N, Benoit G, et al. De novo expression of CD44 in prostate carcinoma is correlated with systemic dissemination of prostate cancer. J Clin Pathol 1998;51:798–802.
24. Desai B, Rogers MJ, Chellaiah MA. Mechanisms of osteopontin and CD44 as metastatic principles in prostate cancer cells. Mol Cancer 2007;6:18.
25. Slack JK, Adams RB, Rovin JD, Bissonette EA, Stoker CE, Parsons JT. Alterations in the focal adhesion kinase/Src signal transduction pathway correlate with increased migratory capacity of prostate carcinoma cells. Oncogene 2001;20:1152–63.
26. Agoulnik IU, Vaid A, Bingman WE III, Erdeme H, Frolov A, Smith CL, et al. Role of SRC-1 in the promotion of prostate cancer cell growth and tumor progression. Cancer Res 2005;65:7959–67.
27. Yuan Y, Mendez R, Sahin A, Dai JL. Hypermethylation leads to silencing of the SYK gene in human breast cancer. Cancer Res 2001;61: 5558–61.
28. Wang L, Duke L, Zhang PS, Arlinghaus RB, Symmans WF, Sahin A, et al. Alternative splicing disrupts a nuclear localization signal in spleen tyrosine kinase that is required for invasion suppression in breast cancer. Cancer Res 2003;63:4724–30.
29. van Weerden WM, de Ridder CM, Verdaasdonk CL, Romijn JC, van der Kwast TH, Schroder FH, et al. Development of seven new human prostate tumor xenograft models and their histopathological characterization. Am J Pathol 1996;149:1055–62.
30. Boormans JL, Korsten H, Ziel-van der Made AJ, van Leenders GJ, de Vos CV, Jenster G, et al. Identification of TDRD1 as a direct target gene of ERG in primary prostate cancer. Int J Cancer 2013;133:335–45.
31. Taylor BS, Schultz N, Hieronymus H, Gopalan A, Xiao Y, Carver BS, et al. Integrative genomic profiling of human prostate cancer. Cancer Cell 2010;18:11–22.
32. Brase JC, Johannes M, Mannsperger H, Fälth M, Metzger J, Kacprzyk LA , et al. TMPRSS2-ERG -specific transcriptional modulation is associated with prostate cancer biomarkers and TGF-β signaling. BMC Cancer 2011; 11:507.
33. Hahn CK, Berchuck JE, Ross KN, Kakoza RM, Clauser K, Schinzel AC, et al. Proteomic and genetic approaches identify Syk as an AML target. Cancer Cell 2009;16:281–94.
34. Floryk D, Tollaksen SL, Giometti CS, Huberman E. Differentiation of human prostate cancer PC-3 cells induced by inhibitors of inosine 5′-monophosphate dehydrogenase. Cancer Res 2004;64:9049–56.
35. Hall CL, Dubyk CW, Riesenberger TA, Shein D, Keller ET, van Golen KL. Type I collagen receptor (alpha2beta1) signaling promotes prostate cancer invasion through RhoC GTPase. Neoplasia 2008;10:797–803.
36. Van Slambrouck S, Hilkens J, Bisoffi M, Steelant WF. AsialoGM1 and integrin alpha2beta1 mediate prostate cancer progression. Int J Oncol 2009;35:693–9.
37. Trerotola M, Rathore S, Goel HL, Li J, Alberti S, Piantelli M, et al. CD133, Trop-2 and alpha2beta1 integrin surface receptors as markers of putative human prostate cancer stem cells. Am J Transl Res 2010;2: 135–44.

Published OnlineFirst November 11, 2014; DOI: 10.1158/0008-5472.CAN-14-0629

38. Fotheringham JA, Coalson NE, Raab-Traub N. Epstein-barr virus latent membrane protein-2A induces ITAM/Syk and Akt dependent epithelial migration through alphaV-integrin membrane translocation. J Virol 2012; 86:10308–20.
39. Woollard KJ, Fisch C, Newby R, Griffiths HR. C-reactive protein mediates CD11b expression in monocytes through the non-receptor tyrosine kinase, Syk, and calcium mobilization but not through cytosolic peroxides. Inflamm Res 2005;54:485–92.
40. Weinblatt ME, Kavanaugh A, Genovese MC, Musser TK, Grossbard EB, Magilavy DB. An oral spleen tyrosine kinase (Syk) inhibitor for rheumatoid arthritis. N Engl J Med 2010;363:1303–12.
41. Baudot AD, Jeandel PY, Mouska X, Maurer U, Tartare-Deckert S, Raynaud SD, et al. The tyrosine kinase Syk regulates the survival of chronic lymphocytic leukemia B cells through PKCdelta and proteasome-dependent regulation of Mcl-1 expression. Oncogene 2009;28: 3261–73.
42. Suljagic M, Longo PG, Bennardo S, Perlas E, Leone G, Laurenti L, et al. The Syk inhibitor fostamatinib disodium (R788) inhibits tumor growth in the Emu-TCL1 transgenic mouse model of CLL by blocking antigen-dependent B-cell receptor signaling. Blood 2010;116:4894–905.
43. Buchner M, Baer C, Prinz G, Dierks C, Burger M, Zenz T, et al. Spleen tyrosine kinase inhibition prevents chemokine- and integrin-mediated stromal protective effects in chronic lymphocytic leukemia. Blood 2010; 115:4497–506.
44. Zhang J, Benavente CA, McEvoy J, Flores-Otero J, Ding L, Chen X, et al. A novel retinoblastoma therapy from genomic and epigenetic analyses. Nature 2012;481:329–34.
45. Spaink HP, Cui C, Wiweger MI, Jansen HJ, Veneman WJ, Marin-Juez R, et al. Robotic injection of zebrafish embryos for high-throughput screening in disease models. Methods 2013;62:246–54.
46. Berton G, Mocsai A, Lowell CA. Src and Syk kinases: key regulators of phagocytic cell activation. Trends Immunol 2005;26:208–14.
47. Dasgupta S, Cushman I, Kpetemey M, Casey PJ, Vishwanatha JK. Prenylated c17orf37 induces filopodia formation to promote cell migration and metastasis. J Biol Chem 2011;286:25935–46.
48. Dasgupta S, Wasson LM, Rauniyar N, Prokai L, Borejdo J, Vishwanatha JK. Novel gene C17orf37 in 17q12 amplicon promotes migration and invasion of prostate cancer cells. Oncogene 2009;28:2860–72.
49. Katz E, Dubois-Marshall S, Sims AH, Faratian D, Li J, Smith ES, et al. A gene on the HER2 amplicon, C35, is an oncogene in breast cancer whose actions are prevented by inhibition of Syk. Br J Cancer 2010;103: 401–10.
50. Leung TH, Wong SC, Chan KK, Chan DW, Cheung AN, Ngan HY. The interaction between C35 and DeltaNp73 promotes chemo-resistance in ovarian cancer cells. Br J Cancer 2013;109:965–75.
51. Hsu CH, Shen TL, Chang CF, Chang YY, Huang LY. Solution structure of the oncogenic MIEN1 protein reveals a thioredoxin-like fold with a redox-active motif. PLoS ONE 2012;7:e52292.
52. Zhou Q, Geahlen RL. The protein-tyrosine kinase Syk interacts with TRAF-interacting protein TRIP in breast epithelial cells. Oncogene 2009;28: 1348–56.
53. Stoletov K, Kato H, Zardouzian E, Kelber J, Yang J, Shattil S, et al. Visualizing extravasation dynamics of metastatic tumor cells. J Cell Sci 2010;123: 2332–41.

Cancer Research
The Journal of Cancer Research (1916–1930) | The American Journal of Cancer (1931–1940)

AACR American Association for Cancer Research

SYK Is a Candidate Kinase Target for the Treatment of Advanced Prostate Cancer

Veerander P.S. Ghotra, Shuning He, Geertje van der Horst, et al.

Cancer Res 2015;75:230-240. Published OnlineFirst November 11, 2014.